Computational Simulation of Temperature Regulation and Vapor Generation Performance of Nicotine Salt Pod System

Wolfgang J. Black[1], Bill Alston[1], Gordon Holloway[1], Jian Tao Zhang[1]
[1]JUUL Labs, Inc., CA, USA

Introduction

The JUUL system is a pre-filled (closed) nicotine salt pod system (NSPS) with automated temperature regulation mechanisms designed to minimize the generation of degradation products and to maintain consistency of temperature. There are no user-modifiable controls.

Purpose

The purpose of this study was to computationally investigate the performance of the NSPS as a function of temperature control, wick material, puff volume, and flow rate with performance criteria of efficiency, vapor generation, and thermal equilibrium.

Methods

An in-house computational fluid dynamics code, EXN/Aero was used to simulate the internal flow and heat transfer within the NSPS. EXN/Aero solves for local velocity, pressure and temperature on a computational mesh of several million elements. It utilizes a SIMPLE numeric solver and can be 1st or 2nd order in time. EXN/Aero has the capability to solve Navier Stokes, Reynolds Averaged Navier Stokes (RANS), and Large Eddy Simulation. Post processing was done using ParaView, an open source multi-platform visualization software developed by Los Alamos National Laboratory.

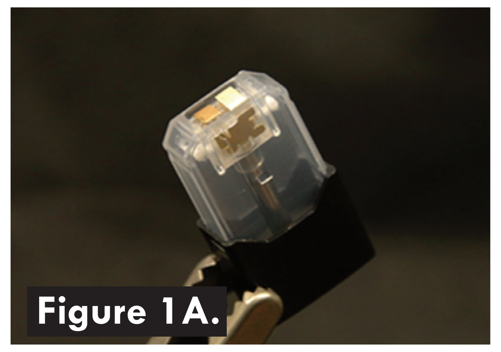

Figure 1A.

Figure 1B.

Figure 1C.

During standard operation, a user puffs on the NSPS pod (**Fig. 1A**), which is inserted into the device. The drop in internal pressure activates the NSPS power circuit. This power circuit employs microprocessor-driven temperature regulation, which utilizes the coil metal target coil resistance, to prevent the wick from exceeding a threshold temperature (300 °C). Once the puff ends, this circuit is shut off and no power is applied to the coil. Various operating parameters were simulated to assess this temperature regulation under different conditions that a user may experience. These conditions include different puff profiles, different volumes, and puff duration (**Fig. 2**), as well as two types of wick materials. The puff profiles were selected with respect to the CORESTA recommended protocol for testing electronic cigarettes, whereas the wick materials represent products currently marketed by JUUL Labs, Inc. in the U.S. and outside of the U.S. Simulations do not consider the total pod geometry; instead they consider the wick, coil, pod inlet, and exit pathway (**Fig. 1B**). A small pod air volume is also considered to represent the airflow pathway. The total simulation domain can be seen in (**Fig. 1C**). Here the wick is white, the coil is copper-colored and the air volume is translucent. Simulations were also run without temperature regulation to show the impact of the NSPS microprocessor-driven temperature control versus non-controlled devices.

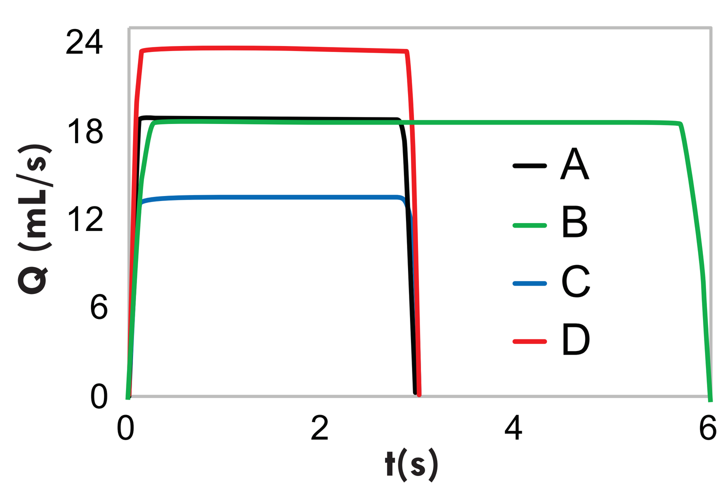

Figure 2. Puff Profiles

Results

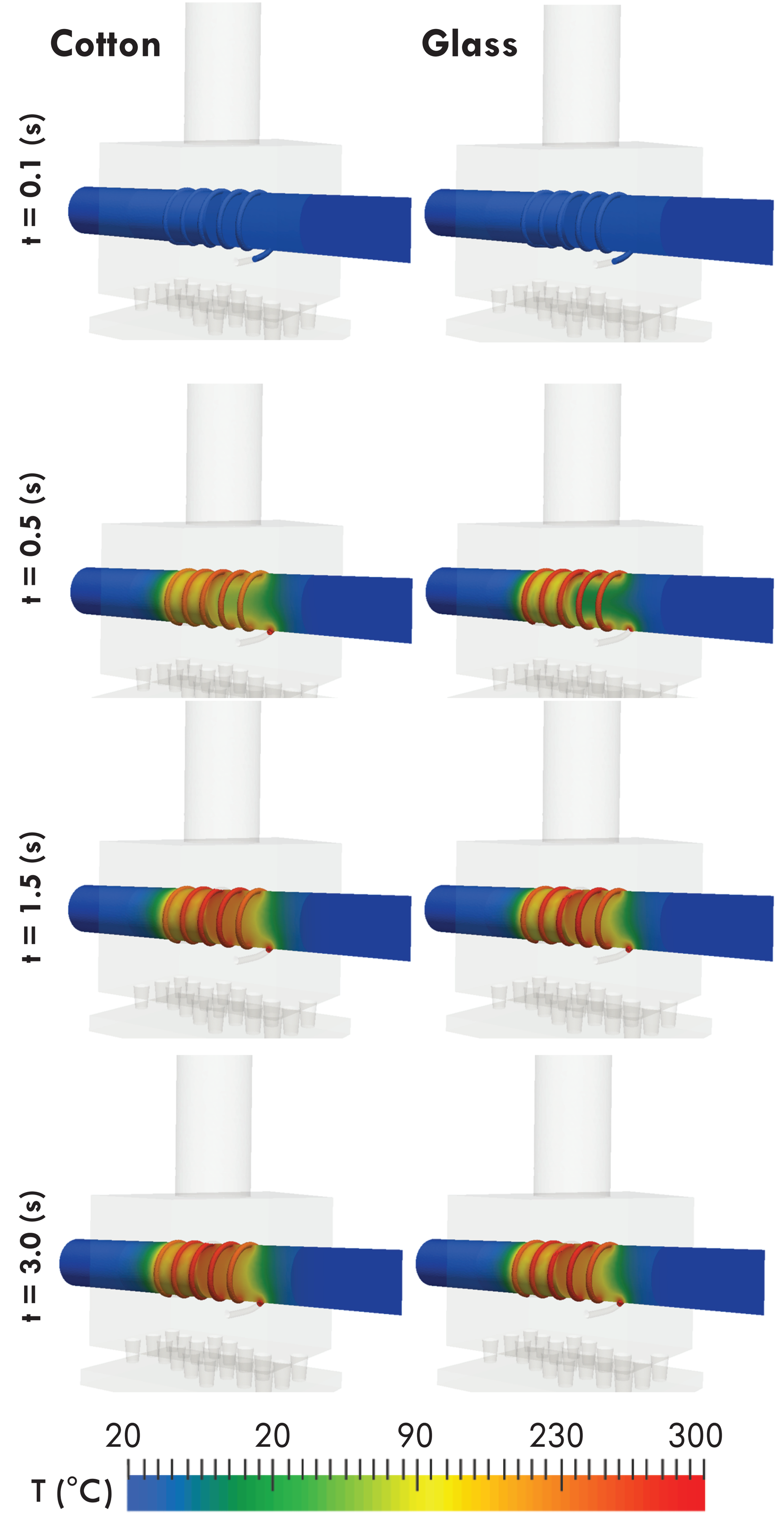

Figure 3. Wick and Coil Temperature with respect to time

Figure 3 shows the thermal evolution of the wick/coil system. The images utilize the flow profile shown in **Fig. 2 (A)** and show both the surface and internal wick/coil temperatures. It can be seen that regardless of the wick material, the temperature of coil remains below 300 °C when in contact with the wick. The max temperature of the coil with temperature regulation is shown in **Fig. 4** to be 300 °C. The surface of the wick near the coil heater can be seen to approach the temperature of the coil, however, the internal temperature is much lower. The glass wick shows higher internal temperature when compared to the cotton wick, which is generally more porous and has a lower thermal conductivity. The temperature of the center of the wick for both materials show a temperature lower than 235 °C.

Figure 4 shows the max coil temperature and the internal wick temperature as a function of time for the glass and cotton wicks at two different flow profiles. Despite having different flow profiles and different timing, the temperature profiles for each material type are consistent.

This consistency of the max coil temperature is due to the microprocessor-driven temperature regulation, which uses the total average resistance rise of the coil to prevent overheating. **Figure 5** shows the simulated max coil temperatures in the absence of temperature regulation. The coil temperatures reach well over 300 °C.

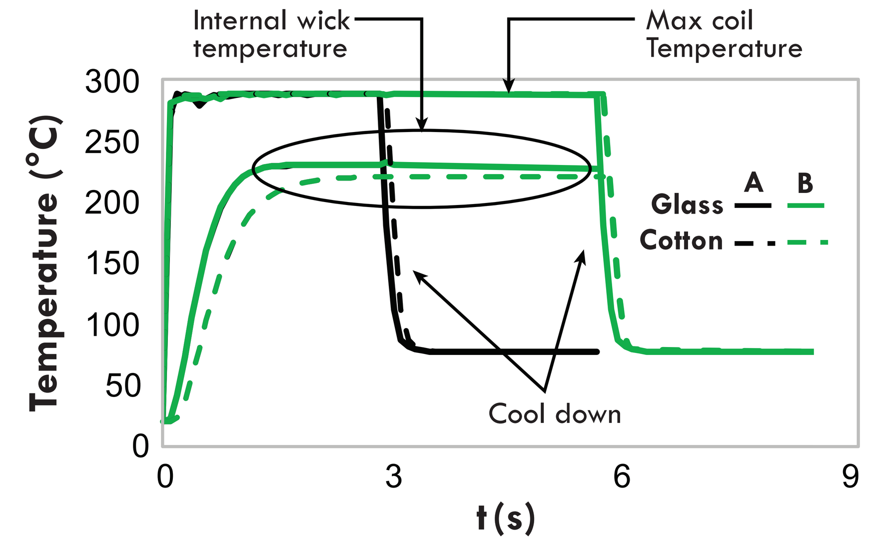

Figure 4. Regulated Temperature

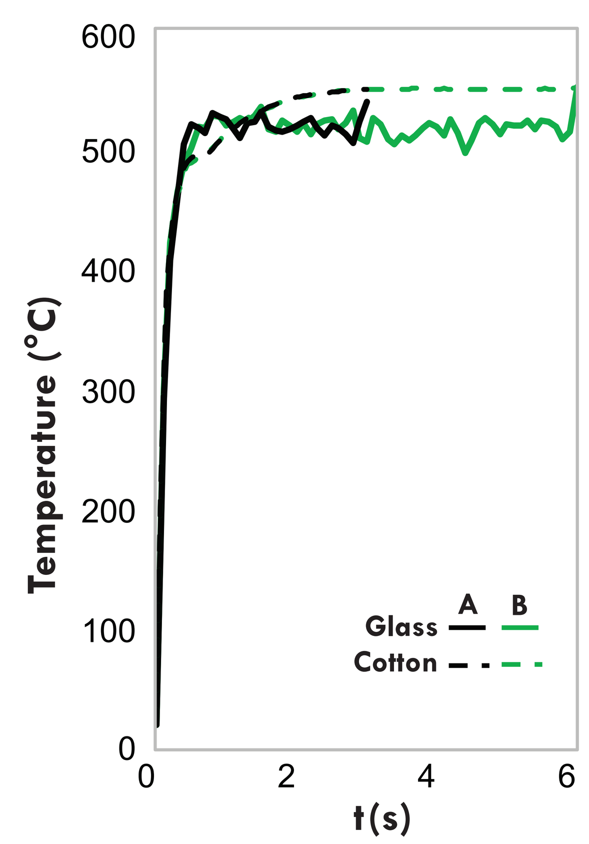

Figure 5. Unregulated Temperature

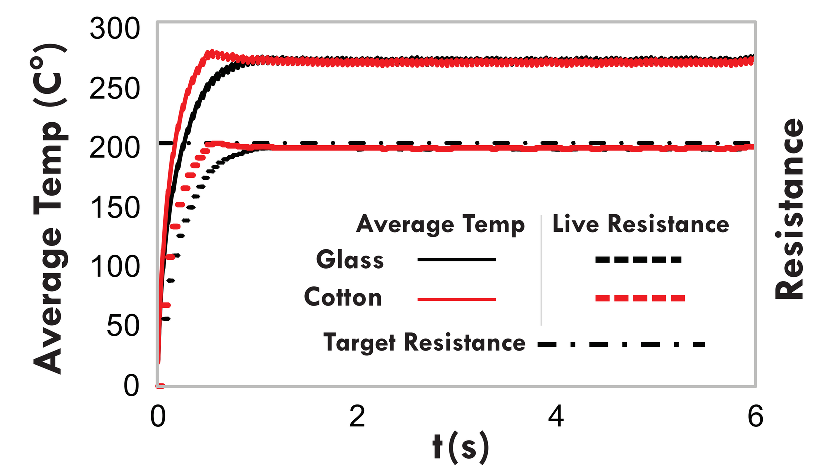

Figure 6. Temperature Regulation

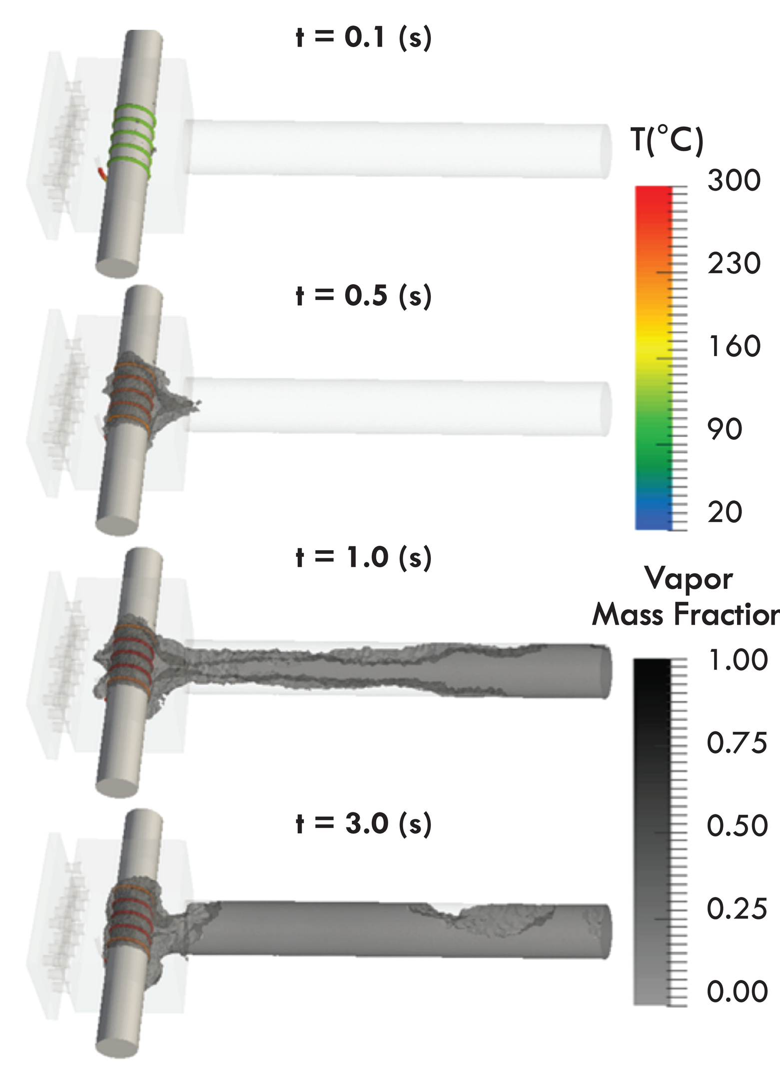

Figure 7. Vapor production with respect to time

It is important to emphasize that this does not occur within the NSPS device either in regulated simulations or in experiments, which utilize the full temperature control. The regulation utilizes the temperature coefficient of resistivity (TCR) curve of the coil metal, the behavior of which is shown in **Fig. 6**.

Figure 6 shows the active temperature regulation simulations utilizing the 6-second puff profile (B) for both the glass and cotton wicks. It can be seen that the live resistance of the coil is sampled (square marked lines) during the simulation and that this resistance is compared to some maximum target resistance (dash-dot-dash line). Using this target resistance to limit the resistance rise of the coil allows for control of the average coil temperature through power regulation. This can be seen in the average temperature profiles (solid lines). The temperature regulation controls for the average coil temperature. This limits the max temperature of the coil in contact with the wick (**Fig. 4**) and prevents these temperatures from exceeding 300 °C. EXN/Aero also computes the vapor production which is shown in **Fig. 7** for a 3-second puff (A) with a glass wick. Here, vapor is visualized in the mesh elements if it is above 5% of the local mass fraction. In this figure, it can be seen that vaporization occurs before 0.5 s, reaches the user before 1 s, and remains steady throughout the remainder of the puff. Aside from timing the vaporization, it can be used to find regions of likely aerosol generation, the total consumed e-liquid mass per puff, and the effects of different puff profiles and temperature regulation on vapor generation.

Conclusions

Simulations have been performed on the NSPS pods with different wick materials, and with puff flow profiles similar to those considered in CORESTA testing. These simulations include the microprocessor-driven temperature control inherent to the NSPS, which employs the coil metal TCR.

These simulations show that both the puff profile and wick material have negligible effect on the maximum coil temperatures. However, the cotton wick shows a lower internal temperature consistent with its lower thermal conductivity. It was also shown that without temperature control, the temperatures of the wick/coil system can exceed 300 °C.